Article

Study on Artificial Neural Network for Predicting Gas-Liquid Two-Phase Pressure Drop in Pipeline-Riser System

Xinping Li [1], Nailiang Li [2], Xiang Lei [2], Ruotong Liu [2], Qiwei Fang [2] and Bin Chen [3,*]

1   School of Mechanics and Civil Engineering, China University of Mining and Technology, Xuzhou 221116, China
2   School of Low-Carbon Energy and Power Engineering, China University of Mining and Technology, Xuzhou 221116, China
3   State Key Laboratory of Multiphase Flow in Power Engineering, Xi'an Jiaotong University, Xi'an 710049, China
*   Correspondence: chenbin@mail.xjtu.edu.cn

Abstract: The pressure drop for air-water two-phase flow in pipeline systems with S-shaped and vertical risers at various inclinations ($-1°$, $-2°$, $-4°$, $-5°$ and $-7°$ from horizontal) was predicted using an artificial neural network (ANN). In the designing of the ANN model, the superficial velocity of gas and liquid as well as the inclination of the downcomer were used as input variables, while pressure drop values of two-phase flows were determined as the output. An ANN network with a hidden layer containing 14 neurons was developed based on a trial-and-error method. A sigmoid function was chosen as the transfer function for the hidden layer, while a linear function was used in the output layer. The Levenberg-Marquardt algorithm was used for the training of the model. A total of 415 experimental data points reported in the literature were collected and used for the creation of the networks. The statistical results showed that the proposed network is capable of calculating the experimental pressure drop dataset with low average absolute percent error (AAPE) of 3.35% and high determination coefficient (R^2) of 0.995.

Keywords: pipeline-riser; gas-liquid; pressure drop; artificial neural network (ANN)

1. Introduction

Gas and liquid two-phase flow is frequently encountered in many processes including petrochemical, chemical, pharmaceutical, power and nuclear engineering. In offshore petroleum fields, the mixture of oil and gas from production wells is usually transported to floating platforms through a pipeline-riser system [1]. Pressure drop is a critical parameter for gas-liquid flows since it is of great importance for the design and operation of pipelines. The subsea pipeline transportation system generally consists of a long-distance pipeline of several kilometers on the seabed, and a riser to the platforms with a length depending on the depth of the water [2]. As a result of the uneven sea bed, the production pipeline transporting oil and gas simultaneously is usually not straight and can vary approximately $-10°$ from the horizontal [3]. A review study by Shao et al. [4] on adiabatic two-phase flows in tubes with different orientations showed that the flow pattern, pressure drop and void fraction are greatly affected by the inclination angle. It is well known that the power consumption costs of pumps constitute a substantial portion of the operational costs for the overall pipeline transportation. Considering the length of the pipeline, the over-estimation of the pressure gradient leads to a huge amount of power being consumed by the pumps. Therefore, a method for the accurate prediction of the pressure drop is required to optimize operational conditions.

It is known that the morphology of the gas-liquid flow greatly effects pressure drop and liquid-holdup [5–7]. A great number of investigations have been performed, and are still ongoing, to gain a better understanding of the flow patterns. The most common

flow regimes found in vertical gas-liquid flows are bubbly flow, churn flow, slug flow, and annular flow [8–11]. To this day, many studies related to the flow patterns of gas-liquid two-phase flow in pipeline-risers have been published. Severe slugging is a typical multiphase flow generated in a pipeline-riser system. Schmidt et al. [12] presented the flow regime diagram of oil and air flowing in the pipeline of 50 mm I.D. Taitel et al. [13] investigated the transition of flow patterns of gas-liquid in pipeline systems with a vertical riser. Based on visual observation and pressure drop over the riser, Malekzadeh et al. [14] observed five typical flow patterns in a long pipeline-riser system. They classified the flow regimes into three types, i.e., unstable oscillating flow, severe slug flow and normal stable flow. As offshore petroleum exploration heads to deep-water, S-shaped risers have been used more and more widely. Tin [15] was the first author to report the results of an experimental investigation on severe slugging occurred in risers with an S-shaped geometry. Five types of unstable flows, including severe slug flow, were recognized in their work. Montgomery [16] performed investigations on air and water in risers with an S-shaped configuration and reported three kinds of unstable flows. Li et al. [17] and, more recently, Li et al. [2] from Xi'an Jiaotong University studied the air-water two-phase flow in an S-shaped flexible riser affected by a long-distance pipeline with 114 m and 1000 m in length, respectively. The flow patterns were classified into two types of severe slug flow and stable flow, which includes normal slug, bubbly and annular flow. Theoretical transition criteria for each flow pattern were also proposed. Based on the current understanding, two-phase flow in complex piping has been paid more and more attention, and studies on the identification of local flow patterns formed in pipeline-risers have been performed by Blaney and Yeung [18] from Cranfield University, and Ye et al. [19], Zou et al. [20] and Xu et al. [21] from Xi'an Jiaotong University. It is evident from the above statement that due to the existence of elbow-connecting pipelines and risers, flow patterns in pipeline-risers are different in comparison with those in tubes with one orientation.

The total pressure drop of gas and liquid flowing in piping generally contains hydrostatic, accelerational, local and frictional pressure drop, among which frictional pressure drop is the most complex term. During the past few decades, much attention has been paid to calculating the two-phase frictional pressure gradient, and many correlations have been proposed. Generally, these models can be regarded as two types, i.e., separated [22–27] and homogeneous flow approaches [28–33]. However, most of these pressure drop prediction models were generated for vertical or horizontal pipes. Therefore, the application of these models is doubtful when they are used for pipeline-riser systems, in which the flow patterns are quite different from those in straight pipes. In addition, the correlations giving satisfactory performance and suitable for estimating the pressure in straight two-phase flows are quite limited. In addition to this, each correlation has its own limitations. For example, some correlations are only applicable to a certain flow regime or a pipe inclination. Spedding and Benard [34] conducted an experimental investigation on the pressure drop of air and water through the 90° bend. It was found that as a result of partial choking by the elbow, the structure of the flow patterns in the upstream vertical tube was quite different to those in straight vertical tubes. Liu et al. [35] studied the fluctuating force induced by a two-phase flow through a 90° elbow with 52.5 mm I.D. and 76.2 mm radius. Kim et al. [36] also conducted a two-phase flow experiment in a horizontal to upwardly vertical pipe connected by a 90-degree bend. The geometric effects of a 90 degrees bend on the pressure drop was investigated. It was found that the conventional Lockhart-Martinelli correlation cannot accurately predict the pressure loss across the elbow due to the fact that the additional loss caused by the flow restrictions was not taken into consideration. They also proposed a new frictional pressure drop correlation by introducing a parameter accounting for the flow restriction configuration into the correlation suggested by Chisholm [23]. More recently, flow patterns and pressure drop of air-water through a complex piping network were experimentally studied by Dang et al. [37]. The piping system of 152.4 mm inner diameter included a horizontal section followed by a downwardly inclined vertical tube of 15.09 m in length and finally ended at a horizontal pipe. Two 90-degree elbows were

used for the connection of pipes with a different orientation. They found that flow restriction geometry notably influences the frictional pressure drop, and the results agree with Kim et al.'s correlation.

The above review indicates that many studies of the two-phase flow in a complex piping system have been conducted and positive results have been obtained. However, only a few results focus on the pressure drop with a flow direction change. It is difficult to predict the pressure drop precisely as a result of the inherent complexity associated with flows having several different phases, especially in piping networks with different inclinations. In offshore petroleum industrial applications, where processes involving gas-liquid two-phase and even gas-liquid-liquid three-phase flows are often formed, the determination of the pressure drop at a specified operating condition is urgently needed for pumping, gathering and transporting oil and gas mixtures. In order to facilitate the design and scale-up of pipelines transporting oil and gas simultaneously, a model that can predict pressure drop with substantial accuracy over a wide range of properties of the working fluid and operating conditions is needed.

Recently, many researchers have demonstrated the successful application of machine learning techniques to overcome the considerable complexity of multiphase flows [38]. ANN is a kind of non-linear and brain-inspired system which tends to behave like a human being [39]. It is suitable for the rapid estimation of process parameters as long as the network is properly trained [39]. Thanks to the advantages of machine learning, one can develop an ANN model even without any knowledge of the process phenomenology [40]. Therefore, ANNs have been used more and more widely for investigating the correlation between processing parameters and final properties [41]. The ability of ANN network to provide accurate results and the requirement for the accurate prediction of pressure drop in complex pipelines inspired this research. The main objective of this study is to develop an ANN model to obtain a sufficiently better prediction of the pressure drop in pipeline conveying gas-liquid with a flow direction change.

2. ANN Model

2.1. Fundamentals of ANN

ANN is a nonlinear tool imitating the human brain. The main features of ANNs are learning adaptation, generalization, massive parallelism, robustness and abstraction. Its abilities for solving complex problems make it a powerful tool for engineering in various applications, including multiphase flow dynamics [42].

The most commonly used is the multi-layer perceptron (MLP), which is composed of input, hidden and output layers. A typical ANN usually consists of input variables, weights, weighted summation and a transfer function, as well as outputs [43]. Input variables are information received by elements in the subsequent layer from the preceding layer. When all inputs are directly obtained through experimental measurement, the ANN is regarded as empirical. If inputs are associated with physical principles, the ANN is semi-empirical. The inputs are multiplied by weights connecting the nodes in adjacent layer. The value of weights is calculated using a fitting procedure. The weighted values of inputs are fed to the summing junction and are summed with the bias of the elements. The summation of the weighted inputs and bias of each element passes through a transfer function and yields output. For a detailed introduction of ANN, the reader might consult references [44].

In practical use, the feed-forward neural network consisting of three layers is the most commonly used network structure [38]. This type of network generally includes an input layer, a hidden layer and an output layer. The first layer of the network acts as a receiver of the input variables from the external environment, while the output of the network is provided by the third layer. Between the input and output layers, there is/are one or more layers named hidden layers. Each of the neurons in the input layer is linked to all of the neurons in the hidden layer, which are also connected to the output neuron. Input variables introduced into the first layer was scaled and propagated to the hidden layer,

where the nodes combine the input from the previous layer and transfer the summation to the output layer.

2.2. ANN Architecture

It is reported that a neural network with one hidden layer is sufficient to produce a satisfactory estimation in most cases [45]. Thus, a three-layer network structure is suggested in the design of a practical feed-forward network. In the present study, a back-propagation network containing one input layer, one hidden layer and one output layer is developed for the prediction of pressure drop over the riser. The structure of the model is illustrated in Figure 1.
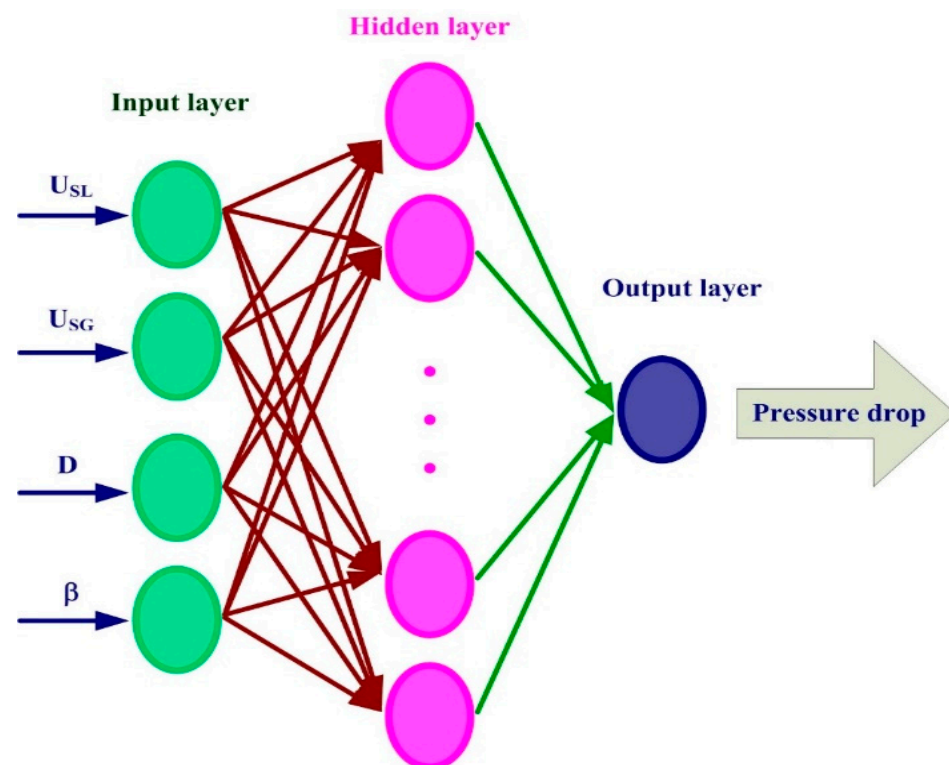
Figure 1. Diagram of the three-layer ANN model developed in the present work.

Physics mechanisms and flow charts are often used for selecting the inputs. More details about the procedure for selecting the input parameters can be found in [46,47]. The input layer has four elements: superficial liquid velocity (U_{SL}), superficial gas velocity (U_{SG}), riser diameter (D) and inclination of downcomer (β). The output of the ANN model has only one variable, i.e., the pressure drop over the riser (Δp). The data in the hidden layer and outlet layer is transferred by a sigmoid function, shown in Equation (1) as follows:

$$z_j = \frac{1}{1 + e^{-y_j}} \tag{1}$$

z_j is the output of jth neuron.

Every single neuron in both the hidden layer and the output layer essentially carries out two tasks: (1) combines all process inputs from the previous layer; and (2) transfers the weighted summation to produce the output to the neurons in the next layer, as is shown in Figure 2.
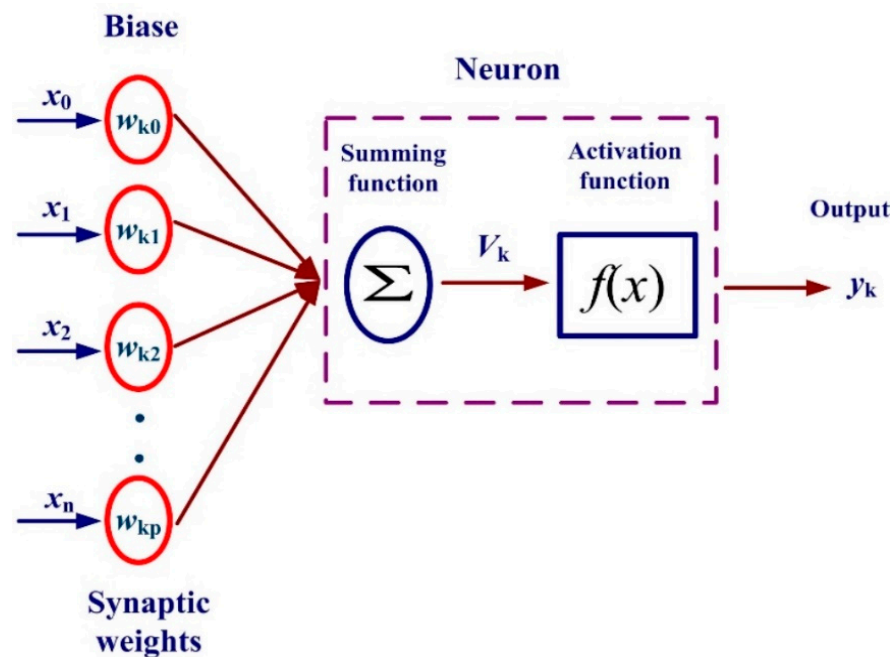
Figure 2. General topology of a single neuron.

In both the hidden layer and the output layer, a weighted summation of all process inputs from the previous layer is produced by each neuron, based on the method given as:

$$y_i = \sum x_i w_{ji} + \theta_j \qquad (2)$$

where y_j is the weighted summation of all the inputs of the *j*th node, x_i represents the output provided by the neuron in the previous layer, the weight between the two linked neurons is w, and θ denotes a threshold value.

The transformation of the weighted summation is accomplished by the activation function. The most frequently used transfer functions in the hidden and output layers are sigmoid and linear. In the present work, Levenberg–Marquardt feed-forward back-propagation algorithms with sigmoid tangent function were used for training the data.

2.3. Training

Before prediction, the ANN needs to be trained on test data to obtain weights that can be used with the same network. In this study, the networks were designed and trained using experimental data points reported by Li et al. [2], Luo et al. [48] and Zhou et al. [49]. A total of three available experimental data sources from a literature search are listed in Table 1, which contains 415 data points and covers both vertical and S-shaped riser flows with a wide range of pipeline inclinations varying from $-1°$ to $-7°$. Details for the dataset, including minimum, maximum, mean and standard deviation, are given in Table 2.

Table 1. Conditions of experimental data collected.

Literature	D (mm)	β (°)	Working Fluids	Riser Hight (m)	Riser Type	U_{SG} (m/s)	U_{SL} (m/s)	Data Point
Li et al. [2]	46	−7	Air, water	11.2	S-shaped	0.06–9.9	0.02–1.0	158
Luo et al. [48]	51	−1, −2, −4	Air, water	4.1	Vertical	0.02–1.0	0.02–1.0	225
Zhou et al. [49]	46	−5	Air, water	16.3	Vertical	0.19–2.5	0.03–1.8	32

Table 2. Details of the entire dataset.

Literature	β (°)	Min (Pa)	Max (Pa)	Mean (Pa)	STD (Pa)
Li et al. [2]	−7	219.5	6347.3	2659.4	1615.2
	−1	243.9	6829.3	3521.9	2028.3
Luo et al. [48]	−2	245.1	7073.2	3480.8	2013.7
	−4	487.1	11,703.3	4452.9	2490.3
Zhou et al. [49]	−5	4192.6	9045.5	7279.1	1452.5

The network training or learning procedure is a process containing iterative calculation in which the network is given the desired inputs along with the correct outputs for specified inputs. During this process, the weights are determined by adjusting itself during each iteration through the training set until the network produces output within a reasonable error margin. The training of the ANN model was performed by using the Levenberg-Marquardt algorithm, which is characterized by fast convergence. The ANN model was trained by the following steps: (1) initialize the weights and calculate the output through the network for a pair of training data chosen randomly; (2) compute the prediction error by the root mean squared (RMS) function; (3) adjust network connection weights and threshold if the error between the predicted and expected output cannot reach a desired value.

The performance of the model is sensitive to the number of neurons designed in the hidden layer. Based on a trial-and-error method, the number of neurons n in the hidden layer can be determined by investigating the behavior of the network through mean squared error (MSE), defined as follows:

$$\text{MSE} = \frac{1}{m}\sum_{i=1}^{m}\left(\Delta P_{Exp,i} - \Delta P_{Cal,i}\right)^2 \tag{3}$$

in which m denotes the total number of data points, ΔP_{Exp} is the pressure drop obtained by means of experiment, ΔP_{cal} is the neural network output representing the predicted pressure drop.

In this study, the range of the number of hidden neurons was tentatively set between 1 and 20. For each number of neurons in the hidden layer, the training process of ANN was performed for 100 times at least, and each case of training cycle produces a training set. Nevertheless, only the ANN model showing the best behavior was chosen as the optimal network with the optimal number of hidden neurons. Thus, the connection weights and biases of each neurons can be determined. The behavior of the network as a function of the neuron number in the hidden layer is shown in Figure 3. It can be observed that the MSE decreases sharply for $n < 5$ and finally stays almost constant at about 0.0005 for n higher than 14. Therefore, the revised number of hidden neurons was determined as 14.

The database of 415 data points was divided into training, validation and testing sets randomly. These three sets account for 70%, 15% and 15% of the entire data points, respectively. The variations of MSE value versus epochs in the process of training of the network with 14 hidden neurons is presented in Figure 4. Curves in blue and red indicate MSE value during training and validation datasets, respectively.

As is seen from Figure 4, a sharp reduction in MSE can be found when epoch is less than 10. For the testing dataset, the best behavior is MSE of 0.0005 at epoch 59, while for training and validation, the MSE value at the same epoch is about 0.0002 and 0.0004, respectively.
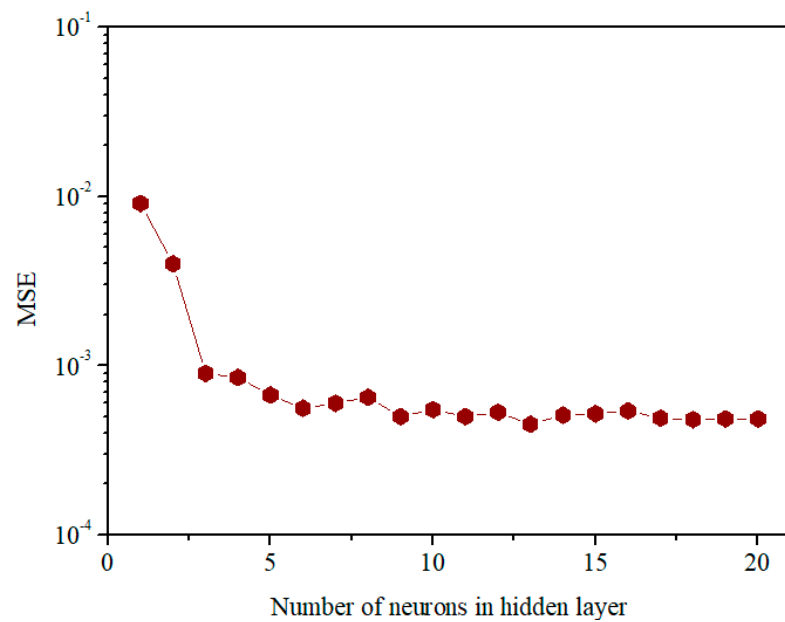
Figure 3. The MSE with respect to the number of neurons in the hidden layer.
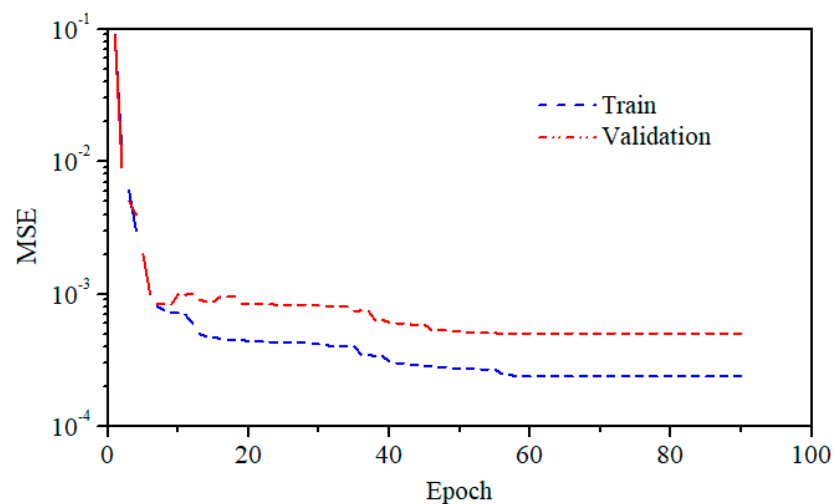
Figure 4. Effect of epochs on MSE in the process of network training.

3. Results and Discussion

Based on the software MATLAB, a three-layer network was developed in which the four inputs are linked to each of the 14 neurons in the hidden layer. A sigmoid function was designed as a transfer function of the hidden layer, while in the output layer a linear function was used. Figures 5–7 compare the ANN output value with training, validation, testing datasets; it is evident that the developed ANN model is able to predict the pressure drop well. The proposed model is valid within the ranges of variables used for training. Comparison of the prediction by the ANN model with experimental pressure drop value of the entire datasets is given in Figure 8. As can be seen, the network model developed in this study yields a good agreement with the datasets of 415 points consisting of the five inclination angles and the two types of riser layout studied.
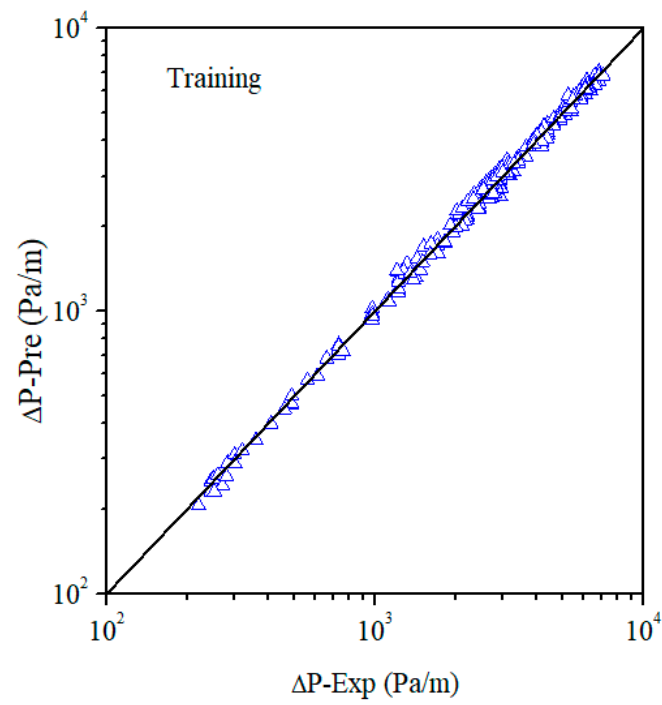
Figure 5. Comparison of predicted pressure drop with experimental values of training dataset.
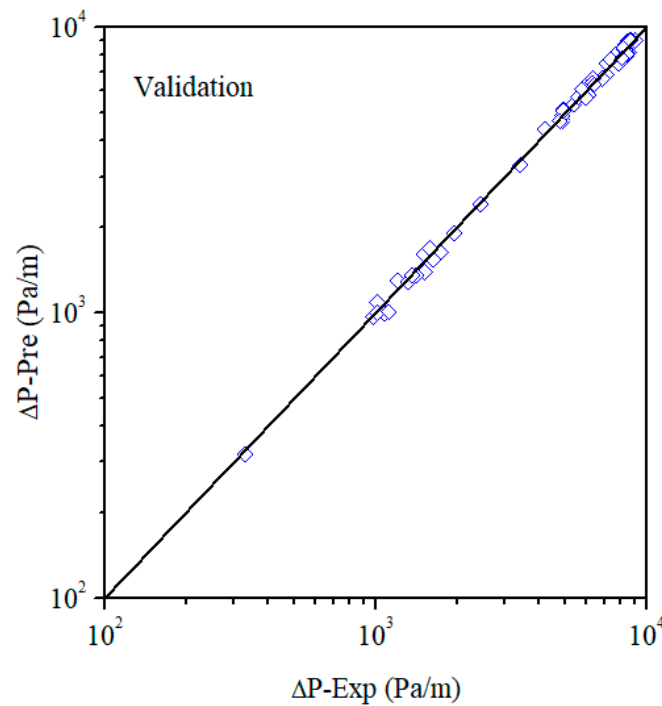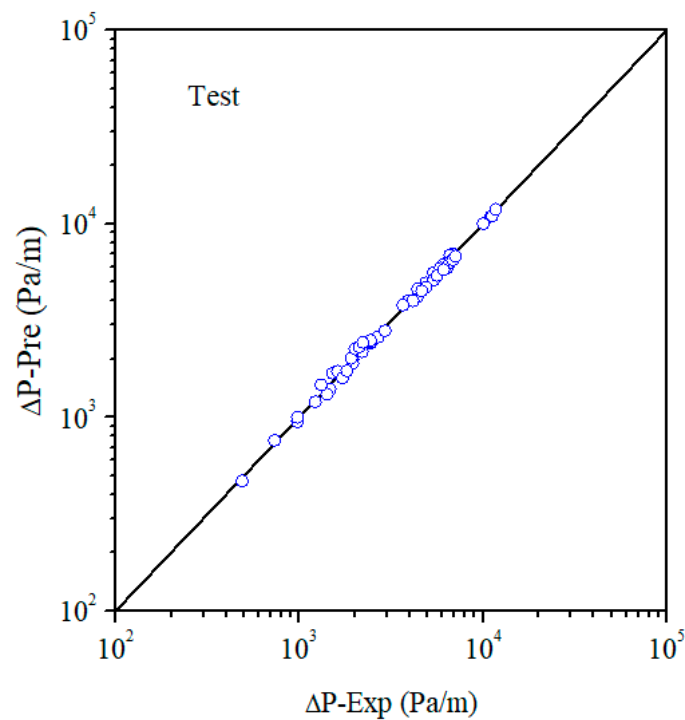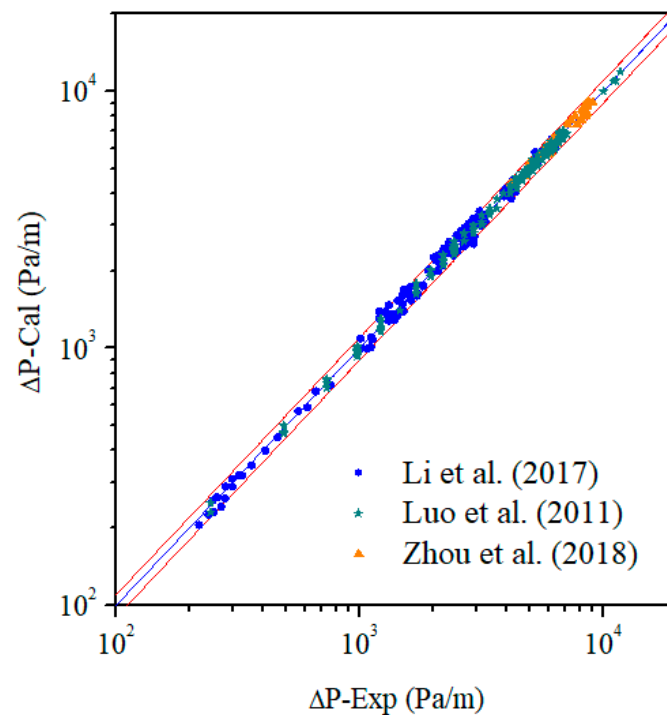

Figure 6. Comparison of predicted pressure drop with experimental values of validation dataset.

Figure 7. Comparison of predicted pressure drop with experimental values of testing dataset.

Figure 8. Comparison of predicted pressure drop with experimental values of dataset reported by Li et al. [2], Luo et al. [48] and Zhou et al. [49].

Determination coefficient of (R^2) as well as mean absolute percent error (AAPE) were calculated to evaluate the optimal network performance. R^2 is defined as:

$$R^2 = 1 - \frac{\sum_{i=1}^{m} \left(\Delta P_{Exp,i} - \Delta P_{Cal,i} \right)^2}{\sum_{i=1}^{m} \left(\Delta P_{Exp,i} - \overline{\Delta P_{Cal}} \right)^2} \tag{4}$$

AAPE is determined according to:

$$\text{AAPE} = \left[\frac{1}{m} \sum_{i=1}^{m} \left| \frac{\Delta P_{Exp,i} - \Delta P_{Cal,i}}{\Delta P_{Exp,i}} \right| \right] \times 100 \tag{5}$$

R^2 and AAPE for training, validation, test and all datasets studied in this work were calculated and the result is illustrated in Table 3. As seen, the neural network performs well, with high R^2 and low AAPE. For the training dataset, AAPE is 2.81% and R^2 is 0.996, while for all the datasets, AAPE and R^2 are 3.35% and 0.995, respectively.

Table 3. Evaluation of the prediction performance of the ANN model developed.

Datasets	R^2	MSE	AAPE (%)	Data Point
Training	0.996	0.00022	2.81	270
Validation	0.991	0.00039	4.08	62
Testing	0.994	0.00031	3.87	83
All	0.995	0.00026	3.35	415

The flow patterns in riser with S-shaped configuration reported by Li et al. [2] were severe slugging, oscillation flow, bubbly flow, churn flow, slug flow and annular flow, covering all the possible flow regimes which occurred in the pipeline-riser system. The flow patterns in vertical risers observed by Luo et al. [48] and Zhou et al. [49] were severe slug flow and transitional severe slug flow. Table 4 compares the results produced by ANN model with the experimental data against different flow regimes. It shows that the results agree with experimental values for most flow patterns in both vertical and S-shaped risers. The highest errors obtained were 5.56% and 7.22% for churn flow and annular flow patterns, respectively, and 4.77% for bubbly flow. Again, an AAPE of 3.35% of the network for all the data points investigated is shown.

Table 4. Performance evaluation of the ANN model prediction against different flow regimes.

Flow Pattern	U_{SG} (m/s)	U_{SL} (m/s)	AAPE (%)	Data Points
Severe slugging	0.02–1.0	0.02–1.0	3.41	290
Transitional flow	0.368–2.46	0.042–0.855	2.32	20
Oscillation flow	0.401	0.794	0.91	31
Bubbly flow	0.062–0.299	0.799–2.1	4.77	9
Slug flow	0.23–1.67	0.79–2.1	3.86	13
Churn flow	1.3–10	0.12–2.1	5.56	43
Annular flow	6.99–10	0.21–0.16	7.22	9
Total	0.02–10	0.022.1	3.35	415

The comparison was made by sorting the data of the experimental pressure drop according to the flow pattern it belongs to. It is also noted that the points for flow patterns are unequal. This is because severe slugging is the most frequent flow patterns. In addition, points for annular flow and bubbly flow are very limited, which might be one of the reasons for the large AAPEs of annular and bubbly flow. The results in Table 4 also indicate that there is a need for more data points, particularly for flow patterns in stable regions.

4. Conclusions

This study presents an accurate artificial neural network (ANN) model for the prediction of pressure drop in pipeline-riser systems. The developed ANN model mainly includes the effects of the inclination angle of downcomer as well as superficial velocities of both liquid and gas phase.

A total of 415 experimental pressure drop data points collected from the literature presented by Li et al. [2] for S-shaped risers and Luo et al. [48] and Zhou et al. [49] for

vertical risers were used for training, validation and testing of the ANN model. All of the data collected were obtained based on experiments performed with air and water. Average absolute percent error (AAPE) as well as determination coefficient (R^2) were calculated to evaluate the performance of the network. The results showed that the ANN model is capable of predicting the data points with a low AAPE of 3.87% and a high R^2 of 0.994 for the testing dataset, and AAPE of 3.35% and R^2 of 0.995 for the entire database. It was demonstrated in this study that the air and water two-phase flow pressure drop in pipeline-risers can be precisely predicted by using artificial neural networks provided the values of the downcomer inclination angle and superficial velocity of gas and liquid phase are determined. In general, the ANN model proposed in the present study has a sufficient accuracy. It is also expected that this trained network has the capability to predict the void fraction for gas-liquid flows in pipeline-riser systems.

References

1. Pedersen, S.; Durdevic, P.; Yang, Z. Challenges in slug modeling and control for offshore oil and gas productions: A review study. *Int. J. Multiph. Flow* **2017**, *88*, 270–284. [CrossRef]
2. Li, W.; Guo, L.; Xie, X. Effects of a long pipeline on severe slugging in an S-shaped riser. *Chem. Eng. Sci.* **2017**, *171*, 379–390. [CrossRef]
3. Amundsen, L. An experimental Study of Oil–Water Flow in Horizontal and Inclined Pipes. Ph.D. Thesis, The Norwegian University of Sciences and Technology, Trondheim, Norway, 2011.
4. Shao, N.; Gavriilidis, A.; Angeli, P. Flow regimes for adiabatic gas–liquid flow in microchannels. *Chem. Eng. Sci.* **2009**, *64*, 2749–2761.
5. Yaqub, M.W.; Marappagounder, R.; Rusli, R.; Prasad, D.M.; Pendyala, R. Review on gas-liquid-liquid three-phase flow patterns, pressure drop, and liquid holdup in pipelines. *Chem. Eng. Res. Des.* **2020**, *159*, 505–528.
6. Wang, B.; Hu, J.G.; Chen, W.X.; Cheng, Z.Z.; Gao, F. Flow pattern and resistance characteristics of gas-liquid two-phase flow with foam under low gas-liquid flow rate. *Energies* **2021**, *14*, 3722.
7. Kumar, A.; Das, G.; Ray, S. Void fraction and pressure drop in gas-liquid downflow through narrow vertical conduits-experiments and analysis. *Chem. Eng. Sci.* **2017**, *171*, 117–130.
8. Brandt, A.; Czernek, K.; Placzek, M.; Witczak, S. Downward annular flow of air-oil-water mixture in a vertical pipe. *Energies* **2021**, *14*, 30. [CrossRef]
9. Chakraborty, S.; Das, P.K. Characterisation and classification of gas-liquid two-phase flow using conductivity probe and multiple optical sensors. *Int. J. Multiph. Flow* **2020**, *124*, 103193.
10. Zhang, Z.; Bieberle, M.; Barthel, F.; Szalinski, L.; Hampel, U. Investigation of upward cocurrent gas-liquid pipe flow using ultrafast x-ray tomography and wire-mesh sensor. *Flow Meas. Instrum.* **2013**, *32*, 111–118.
11. Szalinski, L.; Abdulkareem, L.A.; Da Silva, M.J.; Thiele, S.; Beyer, M.; Lucas, D.; Perez, V.; Hampel, U.; Azzopardi, B.J. Comparative study of gas–oil and gas–water two-phase flow in a vertical pipe. *Chem. Eng. Sci.* **2010**, *65*, 3836–3848.
12. Schmidt, Z.; Doty, D.R.; Dutta-Roy, K. Severe slugging in offshore pipeline riser-pipe systems. *SPE J.* **1985**, *25*, 27–38.
13. Taitel, Y.; Vierkandt, S.; Shoham, O.; Brill, J.P. Severe slugging in a riser system: Experiments and modeling. *Int. J. Multiph. Flow* **2017**, *16*, 57–68. [CrossRef]
14. Malekzadeh, R.; Henkes, R.; Mudde, R.F. Severe slugging in a long pipeline-riser system: Experiments and predictions. *Int. J. Multiph. Flow* **2012**, *46*, 9–21. [CrossRef]
15. Tin, V. Severe slugging in flexible riser. In Proceedings of the 5th International Conference on Multiphase Production, Cannes, France, 1–3 June 1991.
16. Montgomery, J.A. Severe Slugging and Unstable Flows in an S-Shaped Riser. Ph.D. Thesis, Cranfield University, Cranfield, UK, 2002.

17. Li, N.L.; Guo, L.J.; Li, W.S. Gas–liquid two-phase flow regimes in a pipeline–riser system with an S-shaped riser. *Int. J. Multiph. Flow* **2013**, *55*, 1–10.

18. Blaney, S.; Yeung, H. Investigation of the exploitation of a fast-sampling single gamma densitometer and regime recognition to resolve the superficial phase velocities and liquid phase water cut of vertically upward multiphase flows. *Flow Meas. Instrum.* **2008**, *19*, 57–66. [CrossRef]

19. Ye, J.; Guo, L.J. Multiphase flow regime recognition in pipeline–riser system by statistical feature clustering of pressure fluctuations. *Chem. Eng. Sci.* **2013**, *102*, 486–501. [CrossRef]

20. Zou, S.F.; Guo, L.J.; Xie, C. Fast recognition of global flow regime in pipeline-riser system by spatial correlation of differential pressures. *Int. J. Multiph. Flow* **2017**, *88*, 222–237. [CrossRef]

21. Xu, Q.; Li, W.S.; Liu, W.Z.; Zhang, X.M.; Yang, C.Y.; Guo, L.J. Intelligent recognition of severe slugging in a long-distance pipeline-riser system. *Exp. Therm. Fluid Sci.* **2020**, *131*, 110022.

22. Lockhart, R.W.; Martinelli, R.C. Proposed correlation of data for isothermal two phase, two component flow in pipes. *Chem. Eng. Prog.* **1949**, *45*, 39–48.

23. Chisholm, D. Pressure gradients due to the friction during the flow of evaporating two-phase mixtures in smooth tubes and channels. *Int. J. Heat Mass Transf.* **1973**, *16*, 347–358.

24. Kim, W.S.; Lee, J.B.; Kim, K.H. Development of empirical correlation of two-phase pressure drop in moisture separator based on separated flow model. *Energies* **2021**, *14*, 4448.

25. Hoang, H.N.; Agustiarini, N.; Oh, J.T. Experimental investigation of two-phase flow boiling heat transfer coefficient and pressure drop of R448A inside multiport mini-channel tube. *Energies* **2022**, *15*, 4331. [CrossRef]

26. Mishima, K.; Hibiki, T. Some characteristics of air-water two-phase flow in small diameter vertical tubes. *Int. J. Multiph. Flow* **1996**, *22*, 703–712.

27. Yao, C.; Li, H.; Xue, Y.; Liu, X.; Hao, C. Investigation on the frictional pressure drop of gas liquid two-phase flows in vertical downward tubes. *Int. Commun. Heat Mass Transf.* **2018**, *91*, 138–149.

28. McAdams, W.H.; Wood, W.K.; Bryan, R.L. Vaporization inside horizontal tubes. II benzene-oil mixture. *Trans. ASME* **1942**, *66*, 671–684.

29. Akers, W.W.; Deans, A.; Crosssee, O.K. Condensing heat transfer within horizontal tubes. *Chem. Eng. Prog.* **1959**, *55*, 171–176.

30. Dukler, A.E.; Wicks, W.; Cleveland, R.G. Friction pressure drop in two-phase flow. *AICHE J.* **1964**, *10*, 38–43. [CrossRef]

31. Beattie, D.H.; Whalley, P.B. A simple two-phase frictional pressure drop calculation method. *Int. J. Multiph. Flow* **1982**, *8*, 83–87. [CrossRef]

32. Lin, S.; Kwork, C.K.; Li, R.; Chen, Z.; Chen, Z. Local frictional pressure drop during vaporization of R12 through capillary tubes. *Int. J. Multiph. Flow* **1991**, *17*, 95–102.

33. Shannak, B.A. Frictional pressure drop of gas liquid two-phase flow in pipes. *Nucl. Eng. Des.* **2008**, *238*, 3277–3284.

34. Spedding, P.L.; Benard, E. Gas-liquid two phase flow through a vertical 90 elbow bend. *Exp. Therm. Fluid Sci.* **2007**, *31*, 761–769.

35. Liu, Y.; Miwa, S.; Hibiki, T.; Ishii, M.; Morita, H.; Kondoh, Y.; Tanimoto, K. Experimental study of internal two-phase flow induced fluctuating force on a 90 elbow. *Chem. Eng. Sci.* **2012**, *76*, 173–187. [CrossRef]

36. Kim, S.; Kojasoy, G.; Guo, T. Two-phase minor loss in horizontal bubbly flow with elbows: 45 and 90 elbows. *Nucl. Eng. Des.* **2010**, *240*, 284–289.

37. Dang, Z.R.; Yang, Z.J.; Yang, X.H.; Ishii, M. Experimental study on void fraction, pressure drop and flow regime analysis in a large ID piping system. *Int. J. Multiph. Flow* **2019**, *111*, 31–41.

38. Khosravi, A.; Pabon, J.; Koury, R.; Machado, L. Using machine learning algorithms to predict the pressure drop during evaporation of R407C. *Appl. Therm. Eng.* **2018**, *133*, 361–370.

39. Du, X.P.; Chen, Z.J.; Meng, Q.; Song, Y. Experimental analysis and ANN prediction on performances of finned oval-tube heat exchanger under different air inlet angles with limited experimental data. *Open Phys.* **2020**, *18*, 968–980.

40. Soibam, J.; Rabhi, A.; Aslanidou, I.; Kyprianidis, K.; Fdhila, R.B. Derivation and uncertainty quantification of a data-driven subcooled boiling model. *Energies* **2021**, *13*, 5987.

41. Khalaj, G.; Pouraliakbar, H.; Arab, N.; Nazerfakhari, M. Correlation of passivation current density and potential by using chemical composition and corrosion cell characteristics in HSLA steels. *Measurement* **2015**, *75*, 5–11.

42. Khalaj, G.; Pouraliakbar, H.; Mamaghani, K.R.; Khalaj, M.J. Modeling the correlation between heat treatment, chemical composition and bainite fraction of pipeline steels by means of artifcial neural networks. *Neural Netw. World* **2013**, *4*, 351–368.

43. Khalaj, G.; Nazari, A.; Pouraliakbar, H. Prediction of martensite fraction of microalloyed steel by artificial neural networks. *Neural Netw. World* **2013**, *2*, 117–130. [CrossRef]

44. Khalaj, G.; Azimzadegan, T.; Khoeini, M.; Etaat, M. Artificial neural networks application to predict the ultimate tensile strength of X70 pipeline steels. *Neural Comput. Appl.* **2013**, *23*, 2301–2308. [CrossRef]

45. Shirazi, A.S.; Frigaard, I. SlurryNet: Predicting critical velocities and frictional pressure drops in oilfield suspension flows. *Energies* **2021**, *14*, 1263. [CrossRef]

46. Sajjad, U.; Hussain, I.; Hamid, K.; Ali, H.M.; Wang, C.; Yan, W. Liquid-to-vapor phase change heat transfer evaluation and parameter sensitivity analysis of nanoporous surface coatings. *Int. J. Heat Mass Transf.* **2022**, *194*, 123088.

47. Sajjad, U.; Hussain, I.; Raza, W.; Sultan, M.; Alarifi, I.M.; Wang, C. On the Critical Heat Flux Assessment of Micro- and Nanoscale Roughened Surfaces. *Nanomaterials* **2022**, *12*, 3256. [CrossRef]

48.   Luo, X.; He, L.; Ma, H. Flow pattern and pressure fluctuation of severe slugging in pipeline-riser system. *Chin. J. Chem. Eng.* **2011**, *19*, 26–32.

49.   Zhou, H.; Guo, L.; Yan, H.; Kuang, S. Investigation and prediction of severe slugging frequency in pipeline-riser systems. *Chem. Eng. Sci.* **2018**, *184*, 72–84. [CrossRef]